

THE TORSION OF COMPOSITE TUBES AND CYLINDERS

Y. M. KUO and H. D. CONWAY

Cornell University, Ithaca, New York 14850

Abstract—Exact solutions are presented for the Saint-Venant torsion of circular tubes and solid cylinders which are reinforced by cylindrical inclusions of different material equally spaced around a concentric circle. The problems simulate those encountered in matrix rods reinforced by longitudinal fibers, and also in corresponding problems of reinforced concrete. Formulae are obtained for the boundary stress distributions and the torsional rigidities.

Stress function formulations are made for the torsion of cylinders having multiply connected composite sections. Two systems of polar coordinates are employed, and use is made both of periodicity and symmetry. Three degenerate cases—the respective torsion of a homogeneous tube, ring of circular rods and tube with eccentric circular holes—are deduced for checking purposes. Several numerical examples are worked out and the results presented in tabular and graphical forms.

1. INTRODUCTION

COMPOSITE materials in which a relatively weak matrix material is reinforced by stronger fibers have become of increasing technological importance in recent years. When structures fabricated from these materials are loaded, the effect of the relatively stiff fibers is to restrain the deformations of the matrix and correspondingly large stresses may be induced, particularly at the matrix/fiber interfaces. Similar stress and deformation analysis problems are encountered in the design of reinforced concrete structures.

The present investigation is concerned with elastic torsion problems. Although the torsion of homogeneous isotropic prismatic bars has been studied very extensively and by numerous investigators, relatively little work has been done on the corresponding problems of cylinders consisting of two or more different materials bonded together. Muskhelishvili [1] in his well-known book has developed a general formulation for the torsion of composite cylinders in terms of the warping function, and has given two specific examples. These are the circular cylinder reinforced by a single eccentric bar of different material originally solved by Vekua and Rukhadze [2], and the rectangular bar consisting of two different rectangular parts.

Vekua and Rukhadze [3] have also solved the torsion problem of an elliptical rod reinforced by a confocal elliptical bar of different material. The corresponding problem of an elliptical rod with a circular inclusion has been treated by Sherman [4]. Recently Booker and Kitipornchai [5] have developed a method of solution for the technically important problem of multilayered rectangular sections, but only the particular case of two layers has been worked out in detail. The stress function formulation for the torsion of composite material cylinders has been derived by Ely and Zienkiewicz [6], who have worked out three examples by finite difference methods. These examples are a two-layered rectangular cylinder, a square bar with a circular inclusion and a composite cylinder with a circular hole.

The problems mentioned above are either ones in which the cross-sectional boundaries can be mapped conformally with relative ease, or ones in which the warping functions can be expanded quite easily in terms of Fourier series. In contrast to these, Ling [7] has studied the torsion of a circular bar with longitudinal circular holes using a special class of harmonic functions, originally introduced by Howland [8], to take account of the multiple boundaries. Numerical examples have been worked out for 2-hole, 3-hole and 7-hole cases, respectively.

The present article concerns the technically important composite material of a circular rod or tube (the matrix) which is reinforced by a ring of circular cross-section inclusions (the fibers). The problem is also encountered in the torsion of a concrete bar reinforced by longitudinal rods. The stress function for the matrix material is constructed in a manner similar to that used by Ling [7]. The formulation and solution of a reinforced composite tube are given in detail, the case of a reinforced rod being a special case of the former. Perfect bonding is assumed to exist between the two materials and leads to an analysis which is valid for any number of reinforcing inclusions.

2. FORMULATION OF THE BOUNDARY VALUE PROBLEM

Consider a circular tube with outer and inner radii a and δ , respectively. Let it be reinforced by a ring of rods, made of different material, each of radius λ . The centers of the rods are spaced uniformly on a concentric circle of radius, b , as shown in Fig. 1.

The centers of the inclusions may be located in the complex plane by the complex variable

$$z = b e^{2m\pi i/k} \quad (1)$$

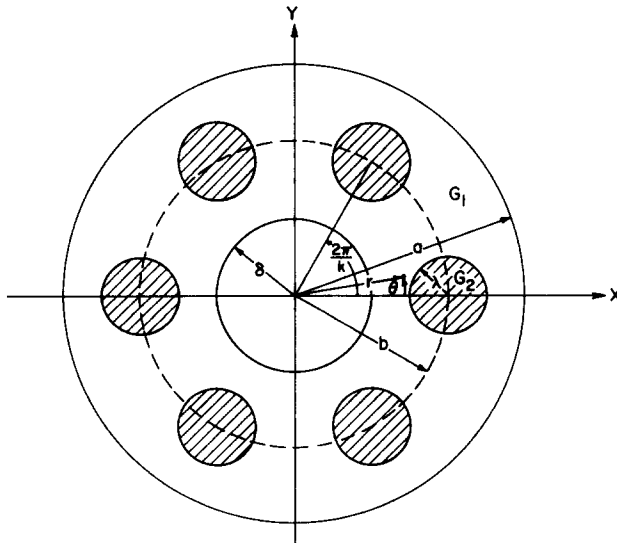


FIG. 1. Circular tube having a ring of circular inclusions.

where b is the distance from the center of the tube to the centers of the inclusions, k is the number of inclusions and $m = 0, 1, \dots, (k-1)$. The origin is taken at the center of the tube.

The tube is made from a material with a shear modulus G_1 and the material of the inclusion has a shear modulus G_2 . It is convenient to introduce the following dimensionless parameters, and these are used throughout the investigation

$$R_1 = \frac{b}{a}, \quad R_2 = \frac{\lambda}{a}, \quad R_3 = \frac{\lambda}{b}, \quad R_4 = \frac{\delta}{a}, \quad R = \frac{G_2}{G_1}. \tag{2}$$

The stress function Φ_1 for the matrix material expressed in terms of polar coordinates (r, θ) must satisfy Poisson's equation

$$\nabla^2 \Phi_1 = \frac{\partial^2 \Phi_1}{\partial r^2} + \frac{1}{r} \frac{\partial \Phi_1}{\partial r} + \frac{1}{r^2} \frac{\partial^2 \Phi_1}{\partial \theta^2} = -2G_1\beta \tag{3}$$

where G_1 is the shear modulus of the matrix material and β is angle of twist per unit length along the axis.

We construct the solution to (3) in the form

$$\Phi_{1(r,\theta)} = -\frac{1}{2}G_1\beta r^2 + G_1\beta a^2 \sum_{n=0}^{\infty} A_n r^{nk} \cos nk\theta + G_1\beta a^2 \sum_{n=1}^{\infty} \frac{B_n}{r^{nk}} \cos nk\theta + G_1\beta a^2 \sum_{s=1}^{\infty} C_s U_s \tag{4}$$

where A_n , B_n and C_s are parametric coefficients to be adjusted so as to satisfy the required boundary conditions. The first term in (4) is a particular solution, and the series with coefficients A_n and B_n are ordinary Fourier series expansions for an annular region.

For the boundary conditions at the matrix inclusion interfaces to be satisfied, another system of harmonic functions with coefficients C_s must be added. Since the system of functions for a homogeneous tube must not have a singularity inside the boundary, therefore the added system must be different in that it possesses singularities inside the tube. Such singularities will eventually be excluded from the matrix material by the inclusions. In our case the inclusions are circular, and it is convenient to place the singularities at the centers of the inclusions. This class of harmonic functions U_s first obtained by Howland [8] and later on used by Ling [7] is defined by

$$W_o = U_o - iV_o = -\log(z^k - b^k) \tag{5}$$

$$W_s = U_s - iV_s = \frac{b^s}{(s-1)!} \frac{d^s W_o}{db^s}.$$

In terms of (r, θ) coordinates we may write

$$U_s = k \sum_{n=1}^{\infty} \binom{nk-1}{s-1} \left(\frac{b}{r}\right)^{nk} \cos nk\theta \quad r > b \tag{6}$$

$$U_s = (-1)^s k \sum_{n=0}^{\infty} \binom{nk+s-1}{s-1} \left(\frac{r}{b}\right)^{nk} \cos nk\theta \quad r < b$$

as shown in the Appendix.

Note that U_o is rejected in (4) because it is a multi-valued function.

Since Φ_1 is symmetrical with respect to the x -axis and periodic in θ with a period $2\pi/k$, we need only consider a segment bounded by $\frac{\pi}{k} \geq \theta \geq -\frac{\pi}{k}$ as shown in Fig. 2.

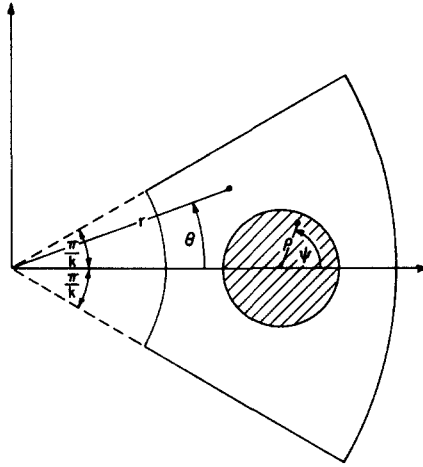


FIG. 2. Segment of shaft bounded by $\frac{\pi}{k} \geq \theta \geq -\frac{\pi}{k}$.

The stress function Φ_2 for the inclusions is expressed in terms of polar coordinates (ρ, ψ) and must satisfy

$$\nabla^2 \Phi_2 = \frac{\partial^2 \Phi_2}{\partial \rho^2} + \frac{1}{\rho} \frac{\partial \Phi_2}{\partial \rho} + \frac{1}{\rho^2} \frac{\partial^2 \Phi_2}{\partial \psi^2} = -2G_2\beta \tag{7}$$

where G_2 is the shear modulus of the inclusion material and β is the angle of twist per unit length defined as before.

Assume

$$\Phi_2(\rho, \psi) = -\frac{1}{2}G_2\beta(b^2 + \rho^2 + 2b\rho \cos \psi) + G_2\beta a^2 \sum_{n=0}^{\infty} D_n \left(\frac{\rho}{\lambda}\right)^n \cos n\psi \tag{8}$$

where the first three terms are particular solutions of the differential equation, and D_n 's are arbitrary constants to be determined by boundary conditions.

The boundary conditions to be satisfied are

$$r = a, \quad \Phi_1 = 0 \tag{9}$$

$$r = \delta, \quad \Phi_1 = \text{constant} = G_1\beta a^2 \Phi_0 \tag{10}$$

where Φ_0 is an undetermined constant.

At the matrix inclusion interfaces $\rho = \lambda$, we have

$$\Phi_1 = \Phi_2 \tag{11}$$

$$\frac{1}{G_1} \frac{\partial \Phi_1}{\partial \rho} = \frac{1}{G_2} \frac{\partial \Phi_2}{\partial \rho} \tag{12}$$

Equation (11) dictates that shear stresses normal to the interfaces be the same in each material, and equation (12) ensures that the axial displacements are compatible on the interfaces.

3. SATISFACTION OF THE BOUNDARY CONDITIONS

To satisfy boundary conditions (9) and (10), Φ_1 is rewritten in the form

$$\begin{aligned} \Phi_{1(r,\theta)} = & -\frac{1}{2}G_1\beta r^2 + G_1\beta a^2 \sum_{n=0}^{\infty} A_n r^{nk} \cos nk\theta + G_1\beta a^2 \sum_{n=1}^{\infty} \frac{B_n}{r^{nk}} \cos nk\theta \\ & + G_1\beta a^2 \begin{cases} \sum_{n=1}^{\infty} \frac{P_n}{r^{nk}} \cos nk\theta, & r > b \\ \sum_{n=0}^{\infty} Q_n r^{nk} \cos nk\theta, & r < b \end{cases} \end{aligned} \tag{13}$$

where

$$P_n = kb^{nk} \sum_{s=1}^{\infty} \binom{nk-1}{s-1} C_s, \quad Q_n = \frac{k}{b^{nk}} \sum_{s=1}^{\infty} (-1)^s \binom{nk+s-1}{s-1} C_s. \tag{14}$$

To apply boundary conditions (11) and (12), we transform Φ_1 in terms of the polar coordinates (ρ, ψ) . Note that

$$r e^{i\theta} = b + \rho e^{i\psi}$$

and

$$\begin{aligned} r^{nk} \cos nk\theta &= \operatorname{Re} \left\{ b^{nk} \left(1 + \frac{\rho}{b} e^{i\psi} \right)^{nk} \right\} = b^{nk} \sum_{m=0}^{nk} \binom{nk}{m} \left(\frac{\rho}{b} \right)^m \cos m\psi \\ r^{-nk} \cos nk\theta &= \operatorname{Re} \left\{ b^{-nk} \left(1 + \frac{\rho}{b} e^{i\psi} \right)^{-nk} \right\} = \frac{1}{b^{nk}} \sum_{m=0}^{\infty} (-1)^m \binom{nk+m-1}{m} \left(\frac{\rho}{b} \right)^m \cos m\psi \end{aligned}$$

also

$$r^2 = b^2 + \rho^2 + 2b\rho \cos \psi.$$

Thus

$$\begin{aligned} \Phi_{1(\rho,\psi)} = & -\frac{1}{2}G_1\beta(b^2 + \rho^2 + 2b\rho \cos \psi) + G_1\beta a^2 \sum_{m=0}^{\infty} M_m \left(\frac{\rho}{b} \right)^m \cos m\psi \\ & + G_1\beta a^2 \sum_{m=0}^{\infty} N_m \left(\frac{\rho}{b} \right)^m \cos m\psi + G_1\beta a^2 \left\{ L_o + \sum_{m=1}^{\infty} \left(C_m \frac{b^m}{\rho^m} + L_m \frac{\rho^m}{b^m} \right) \cos m\psi \right\} \end{aligned} \tag{15}$$

where

$$\begin{aligned} M_m &= \sum_{n=0}^{\infty} \binom{nk}{m} R_1^{nk} A_n a^{nk} \\ N_m &= (-1)^m \sum_{n=1}^{\infty} \binom{nk+m-1}{m} \frac{1}{R_1^{nk}} \frac{B_n}{a^{nk}} \\ L_m &= (-1)^m \sum_{s=1}^{\infty} {}^m\alpha_s C_s. \end{aligned} \tag{16}$$

See Appendix for $\sum_{s=1}^{\infty} C_s U_s$ in (ρ, ψ) coordinates.

Application of all the boundary conditions then leads to the following relations

$$\begin{aligned}
 A_o &= \frac{1}{2} \\
 A_n a^{nk} &= \left(Q_n a^{nk} R_4^{2nk} - \frac{P_n}{a^{nk}} \right) / (1 - R_4^{2nk}) \\
 \frac{B_n}{a^{nk}} &= R_4^{2nk} \left(\frac{P_n}{a^{nk}} - Q_n a^{nk} \right) / (1 - R_4^{2nk}) \\
 \Phi_o &= Q_o + \frac{1}{2}(1 - R_4^2) \\
 D_o &= \frac{M_o + N_o + L_o}{R} + \frac{R-1}{2R}(R_1^2 + R_2^2) \\
 D_1 &= R_1^2 R_3^2 - \frac{2C_1}{R_3(1-R)} \\
 D_m &= \frac{2C_m}{(R-1)R_3^m}, \quad m \geq 2.
 \end{aligned}
 \tag{16}$$

From the above equations, with the aid of (14) and (16), we can express all the coefficients in terms of C_n 's. The equations for the solution of C_n 's are seen to be

$$\begin{aligned}
 R_3^2 \sum_{n=1}^{\infty} E_n^1 C_n &= \frac{R+1}{R-1} C_1 + R_2^2 \\
 R_3^{2m} \sum_{n=1}^{\infty} E_n^m C_n &= \frac{R+1}{R-1} C_m, \quad m \geq 2
 \end{aligned}
 \tag{17}$$

where

$$\begin{aligned}
 E_n^m &= (-1)^m m \alpha_n + k \sum_{l=1}^{\infty} \left\{ \frac{R_1^{2lk}}{1 - R_4^{2lk}} \binom{lk}{m} \left[(-1)^n \left(\frac{R_4}{R_1} \right)^{2lk} \binom{lk+n-1}{n-1} - \binom{lk-1}{n-1} \right] \right. \\
 &\quad \left. + \frac{(-1)^m R_4^{2lk}}{(1 - R_4^{2lk}) R_1^{2lk}} \binom{lk+m-1}{m} \left[R_1^{2lk} \binom{lk-1}{n-1} - (-1)^n \binom{lk+n-1}{n-1} \right] \right\}.
 \end{aligned}$$

Equation (17) is an infinite system of linear equations which may be truncated and solved by machine computation.

4. BOUNDARY STRESS DISTRIBUTIONS

Let $\tau_{zr}, z_{z\theta}$ denote, respectively, the radial and tangential stresses in the coordinates (r, θ) and $\tau_{z\rho}, \tau_{z\psi}$ the radial and tangential stresses in the coordinates (ρ, ψ) . Subscript "1" will imply that the stresses are in the matrix and subscript "2" that the stresses are in the inclusion material.

(i) On the boundary $r = a$

$$(\tau_{z\theta})_1 = \left(-\frac{\partial \Phi_1}{\partial r} \right)_{r=a} = G_1 \beta a \left[1 - 2k \sum_{n=1}^{\infty} n(A_n a^{nk}) \cos nk\theta \right]
 \tag{18}$$

(ii) On the boundary $r = \delta$

$$(\tau_{z\theta})_1 = \left(-\frac{\partial\Phi_1}{\partial r} \right)_{r=\delta} = G_1\beta a \left[R_4 + \frac{2k}{R_4} \sum_{n=1}^{\infty} \frac{n}{R_4^{nk}} \frac{B_n}{a^{nk}} \cos nk\theta \right] \tag{19}$$

(iii) On the boundary $\rho = \lambda$

$$(\tau_{z\rho})_1 = \left(\frac{1}{\rho} \frac{\partial\Phi_1}{\partial\rho} \right)_{\rho=\lambda} = G_1\beta a \left(-\frac{2R}{R-1} \sum_{m=1}^{\infty} \frac{m}{R_1 R_3^{m+1}} C_m \sin m\psi \right) \tag{20}$$

$$(\tau_{z\psi})_1 = \left(-\frac{\partial\Phi_1}{\partial\rho} \right)_{\rho=\lambda} = G_1\beta a \left(R_2 - \frac{2}{R-1} \sum_{m=1}^{\infty} \frac{m}{R_1 R_3^{m+1}} C_m \cos m\psi \right) \tag{21}$$

$$(\tau_{z\rho})_2 = \left(\frac{1}{\rho} \frac{\partial\Phi_2}{\partial\rho} \right)_{\rho=\lambda} = G_1\beta a \left(-\frac{2R}{R-1} \sum_{m=1}^{\infty} \frac{m}{R_1 R_3^{m+1}} C_m \sin m\psi \right) \tag{22}$$

$$(\tau_{z\psi})_2 = \left(-\frac{\partial\Phi_2}{\partial\rho} \right)_{\rho=\lambda} = G_1\beta a R \left(R_2 - \frac{2}{R-1} \sum_{m=1}^{\infty} \frac{m}{R_1 R_3^{m+1}} C_m \cos m\psi \right). \tag{23}$$

5. TORSIONAL RIGIDITY AND EFFECTIVE SHEAR MODULUS

The twisting moment can be evaluated by

$$T = 2k \left[2 \int_{S_1} \Phi_1 dS_1 + 2 \int_{S_2} \Phi_2 dS_2 \right] + 2\pi\delta^2(G_1\beta a^2\Phi_o)$$

where S_1 is the area shown in Fig. 3 excluding S_2 . The area S_1 is $1/(2k)$ times the total area of the tube excluding all the inclusions, and S_2 is one half of the cross-sectional area of an inclusion.

Substituting for Φ_1 and Φ_2 in the above expression and integrating term by term, we obtain

$$\begin{aligned} T = & -\frac{\pi}{2}G_1\beta(a^4 - \delta^4) + \pi G_1\beta a^2(a^2 - \delta^2) + 2\pi\delta^2 G_1\beta a^2\Phi_o \\ & + kG_1\beta b^2\lambda^2\pi + \frac{\pi}{2}kG_1\beta\lambda^4 - 2k\pi\lambda^2 G_1\beta a^2(M_o + N_o) \\ & - k\pi\lambda^2 G_2\beta b^2 - \frac{k}{2}\pi G_2\beta\lambda^4 + 2k\pi\lambda^2 G_2\beta a^2 D_o - 2k\pi\lambda b G_1\beta a^2 C_1. \end{aligned} \tag{24}$$

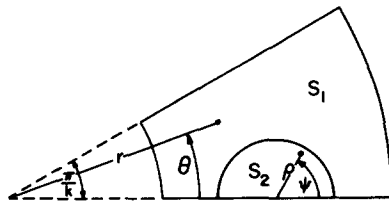


FIG. 3. $1/(2k)$ of the total cross-sectional area.

It is convenient to introduce an effective shear modulus G_e defined by

$$G_e = \frac{T}{\frac{\pi}{2}\beta(a^4 - \delta^4)} \tag{25}$$

where T is given by (24). Substituting for T in (25) and writing in dimensionless form, it follows that

$$\frac{G_e}{G_1} = \frac{T}{\frac{\pi}{2}G_1\beta(a^4 - \delta^4)} = \left[(1 - R_4^2)^2 + 4R_4^2\Phi_o + 2kR_2^2(1 - R)\left(R_1^2 + \frac{R_2^2}{2}\right) + 4kR_2^2(D_oR - M_o - N_o) - 4kR_1R_2C_1 \right] (1 - R_4^4). \tag{26}$$

6. DEGENERATE CASES

(i) $G_1 = G_2 = G, \text{ or } R = 1.$

For this case, the following equations are found

$$\begin{aligned} Q_o &= 0; & P_n &= Q_n = 0, & n &\geq 1 \\ A_n a^{nk} &= \frac{B_n}{a^{nk}} = 0, & n &\geq 1 \\ \Phi_o &= \frac{1}{2}(1 - R_4^2) \\ M_o &= D_o = \frac{1}{2}; & N_a &= L_o = 0 \\ M_m &= N_m = L_m = 0, & m &\geq 1. \end{aligned}$$

Substituting all these values in (18), (19) and (24), we obtain

$$\begin{aligned} (\tau_{z\theta})_1 &= G\beta a \text{ at } r = a \\ (\tau_{z\theta})_1 &= G\beta\delta \text{ at } r = \delta \end{aligned}$$

and

$$\frac{T}{G_1\beta a^4} = \frac{\pi}{2}(1 - R_4^4).$$

This is the solution for the torsion of a homogeneous tube.

(ii) $G_1 = 0, \text{ or } R = \infty.$

Equation (23) gives

$$(\tau_{z\psi})_2 = G_2\beta a R_2 = G_2\beta\lambda \text{ at } \rho = \lambda.$$

Equation (24) gives

$$T = \frac{\pi}{2}kG_2\beta\lambda^4.$$

This is the torsion solution for a ring of k bars.

(iii) $G_2 = 0, \text{ or } R = 0$

We have from (18), (19) and (21)

$$\begin{aligned}
 (\tau_{z\theta})_1 &= G_1\beta a \left[1 - 2k \sum_{n=1}^{\infty} n(A_n a^{nk}) \cos nk\theta \right] \quad \text{at } r = a \\
 (\tau_{z\theta})_1 &= G_1\beta a \left[R_4 + \frac{2k}{R_4} \sum_{n=1}^{\infty} \frac{n}{R_4^{nk}} \frac{B_n}{a^{nk}} \cos nk\theta \right] \quad \text{at } r = \delta \\
 (\tau_{z\psi})_1 &= G_1\beta a \left[R_2 + 2 \sum_{m=1}^{\infty} \frac{m}{R_1 R_3^{m+1}} C_m \cos m\psi \right] \quad \text{at } \rho = \lambda.
 \end{aligned}$$

From (24) we obtain

$$\frac{T}{G_1\beta a^4} = \frac{\pi}{2}(1 - R_4^2) + 2\pi R_4^2\Phi_o + k\pi R_2^2 \left(R_1^2 + \frac{R_2^2}{2} \right) + 2k\pi R_2^2(D_oR - M_o - N_o) - 2k\pi R_1 R_2 C_1$$

where

$$\Phi_o = Q_o + \frac{1}{2}(1 - R_4^2)$$

and

$$D_oR = M_o + N_o + L_o - \frac{1}{2}(R_1^2 + R_2^2).$$

This is the torsion solution for a circular tube with longitudinal circular holes which was solved by Ling [7]. Note that $(M_o + N_o)$ is set approximately equal to $\frac{1}{2}$ in Ling's paper.

7. NUMERICAL RESULTS AND DISCUSSIONS

A computer program based on the foregoing analysis has been written and the numerical results have been obtained by machine computation. As illustrated, the torsional rigidities and boundary stress distribution for the following three cases are obtained and given in tabular and graphical forms:

- (i) $\frac{b}{a} = \frac{3}{4}, \quad \frac{\lambda}{a} = \frac{1}{8}, \quad \frac{\delta}{a} = \frac{1}{2}, \quad \frac{G_2}{G_1} = 30, \quad k = 8,$
- (ii) $\frac{b}{a} = \frac{3}{4}, \quad \frac{\lambda}{a} = \frac{1}{8}, \quad \frac{\delta}{a} = \frac{1}{2}, \quad \frac{G_2}{G_1} = 5, \quad k = 3,$
- (iii) $\frac{b}{a} = \frac{1}{2}, \quad \frac{\lambda}{a} = \frac{1}{4}, \quad \frac{\delta}{a} = 0, \quad \frac{G_2}{G_1} = 30, \quad k = 4.$

These cases represent, respectively, a tube reinforced by eight relatively rigid fiber inclusions, a tube reinforced by three relatively flexible inclusions and a solid cylinder having four large rigid inclusions.

The effective shear moduli ratios for the above three cases are given in Table 1. As a partial experimental verification a torsion test was carried out on a solid 1 in. dia. epoxy rod reinforced by four $\frac{1}{4}$ in. dia. brass rods corresponding to case (iii) above. The shear moduli obtained from torsion tests on completely epoxy and brass bars were 170,000 and 5×10^6 psi, respectively, and thus $\frac{G_2}{G_1} = 29.4$. The value of $\frac{G_e}{G_1}$ obtained from the torsion test on the reinforced rod was 1.53, and this agrees very well indeed with the theoretical value of 1.57 given in Table 1.

TABLE 1. EFFECTIVE SHEAR MODULUS RATIO $\frac{G_e}{G_1}$

	$\frac{b}{a}$	$\frac{\lambda}{a}$	$\frac{\delta}{a}$	$\frac{G_2}{G_1}$	k	$\frac{G_e}{G_1}$
Case (i)	$\frac{3}{4}$	$\frac{1}{8}$	$\frac{1}{2}$	30	8	1.2330
Case (ii)	$\frac{3}{4}$	$\frac{1}{8}$	$\frac{1}{2}$	5	3	1.0466
Case (iii)	$\frac{1}{2}$	$\frac{1}{4}$	0	30	4	1.5706

The boundary shear stress distributions for the above three cases were computed and are shown in Figs. 4, 5 and 6, respectively. It will be observed that the tangential shear stresses $(\tau_{z\theta})_1$ on the inner boundaries $r = \delta$ always have minimum values at $\theta = 0$, that is, at points nearest the inclusions. These stresses increase as θ increases, reaching maximum values at $= \frac{\pi}{k}$, that is at points at greatest distances from the inclusions.

In the matrix, the boundary shear stresses normal to the matrix/inclusion interfaces are bigger than those tangential to the interfaces. This statement may or may not be so for the stresses in the inclusion depending on the $\frac{G_2}{G_1}$ ratio.

It would appear that the shear stresses $(\tau_{z\rho})_1$ and $(\tau_{z\rho})_2$ normal to the interfaces attain maximum values at $\psi \geq 90^\circ$, and are zero at $\psi = 0$ and 180° . The stresses $(\tau_{z\psi})_1$ and $(\tau_{z\psi})_2$ tangential to the interfaces have maximum values at $\psi = 0^\circ$, and decrease gradually as ψ increases; they may have negative values if G_2 is not much bigger than G_1 as shown in Fig. 5.

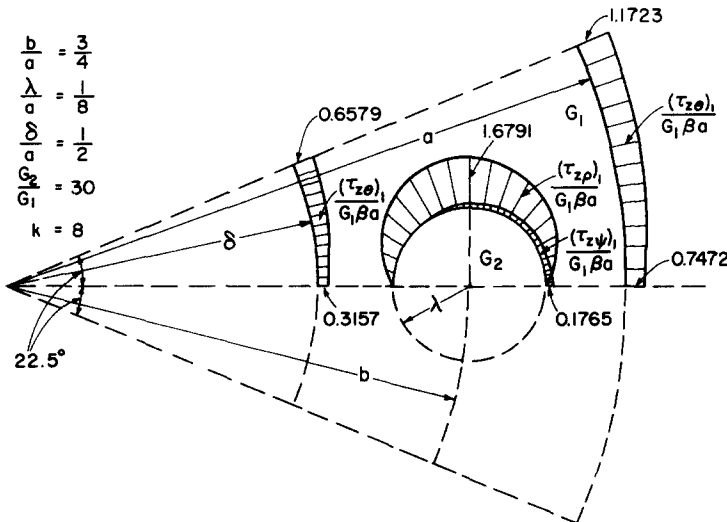


FIG. 4. Boundary stress distributions $\left(\frac{b}{a} = \frac{3}{4}, \frac{\lambda}{a} = \frac{1}{8}, \frac{\delta}{a} = \frac{1}{2}, \frac{G_2}{G_1} = 30, k = 8 \right)$.

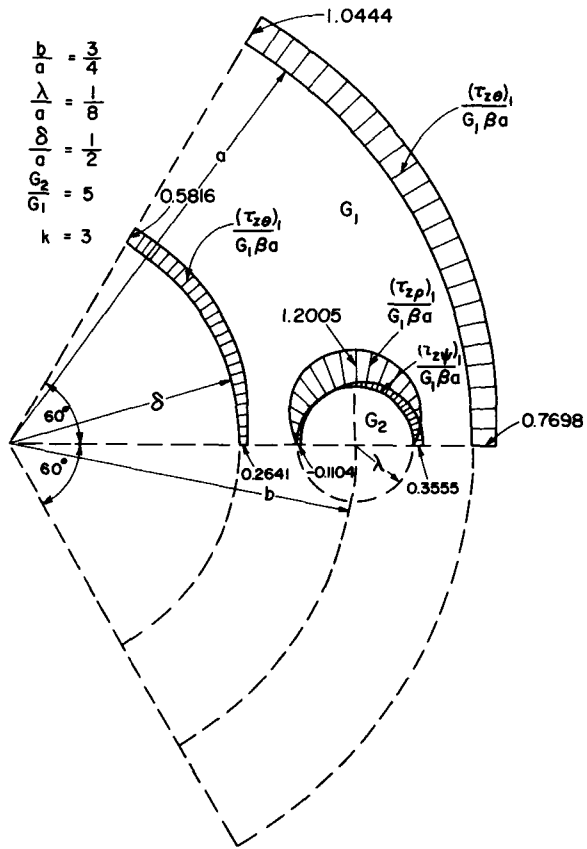


FIG. 5. Boundary stress distributions $\left(\frac{b}{a} = \frac{3}{4}, \frac{\lambda}{a} = \frac{1}{8}, \frac{\delta}{a} = \frac{1}{2}, \frac{G_2}{G_1} = 5, k = 3\right)$.

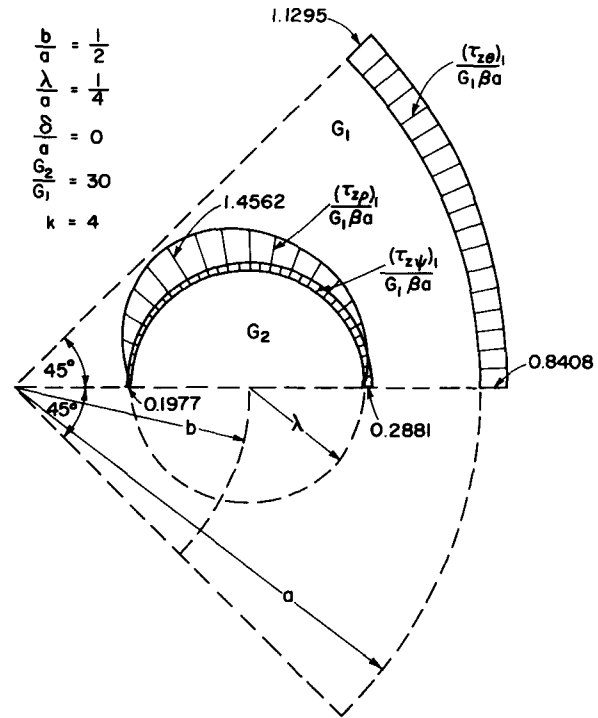


FIG. 6. Boundary stress distributions $\left(\frac{b}{a} = \frac{1}{2}, \frac{\lambda}{a} = \frac{1}{4}, \frac{\delta}{a} = 0, \frac{G_2}{G_1} = 30, k = 4\right)$

It might appear that the greatest boundary stress in the matrix occurs on $\rho = \lambda$. However, additional calculations have shown that such is not always the case. For example, when

$$\frac{b}{a} = \frac{1}{2}, \quad \frac{\lambda}{a} = \frac{1}{4}, \quad \frac{\delta}{a} = 0, \quad \frac{G_2}{G_1} = 5 \quad \text{and} \quad k = 3$$

the greatest boundary matrix stress occurs on $r = a$.

Acknowledgement—The results presented here form part of a continuing program of research on the bond stresses and displacement in composite materials. The financial support of the Advanced Research Projects Agency and the National Science Foundation (Grant GH 33637) through the Materials Science Center, Cornell University, is gratefully acknowledged.

REFERENCES

- [1] N. I. MUSKHELISHVILI, *Some Basic Problems of the Mathematical Theory of Elasticity*. Noordhoff (1953).
- [2] I. N. VEKUA and A. K. RUKHADZE, The problem of torsion of a circular cylinder, reinforced by additional circular rods. *Izv. A.N.S.S.S.R.* No. 3 (1933).
- [3] I. N. VEKUA and A. K. RUKHADZE, Torsion and bending by a transverse force of a bar, consisting of two materials bounded by confocal ellipses. *Prikl. Mat. Mech.* I (2) (1933).
- [4] D. I. SHERMAN, Torsion of an elliptical cylinder reinforced by a circular rod. *Inzhenernyi Sbornik*, 10 (1951).
- [5] JOHN R. BOOKER and S. KITIPORNCHAI, Torsion of multilayered rectangular section. *ASCE Engng Mech. Div.* 97 (EM5) (1971).
- [6] J. F. ELY and O. C. ZIENKIEWICZ, Torsion of compound bars—A relaxation solution. *Int. J. Mech. Sci.* 1 (4) (1960).
- [7] C. B. LING, Torsion of a circular tube with longitudinal circular holes. *Q. Appl. Math.* 5 (2) (1947).
- [8] R. C. J. HOWLAND, Potential functions with periodicity in one coordinate. *Proc. Camb. Phil. Soc.* 30 (1934).

APPENDIX

A class of harmonic functions for a ring of circular boundaries

Consider the z plane with a series of k points located by

$$z = b e^{2m\pi i/k} \tag{A1}$$

where $m = 0, 1, 2, \dots, (k-1)$

A function with a logarithmic singularity at each such point is defined by

$$W_o = -\log(z^k - b^k). \tag{A2}$$

The power series expansion of W_o about $z = 0$ according to $|z| > b$ and $|z| < b$ is constructed in the following manner

$$W_o = -\log z^k \left(1 - \frac{b^k}{z^k}\right) = -k \log z + \sum_{n=1}^{\infty} \frac{1}{n} \left(\frac{b}{z}\right)^{nk}, \quad |z| > b \tag{A3}$$

and

$$W_o = -\log \left[e^{-i\pi} b^k \left(1 - \frac{z^k}{b^k}\right) \right] = i\pi - k \log b + \sum_{n=1}^{\infty} \frac{1}{n} \left(\frac{z}{b}\right)^{nk}, \quad |z| < b \tag{A4}$$

where W_s is defined as

$$W_s = \frac{b^s}{(s-1)!} \frac{d^s W_o}{db^s}. \tag{A5}$$

Differentiating (A3) and (A4) s times and substituting in (A5), we obtain

$$W_s = k \sum_{n=1}^{\infty} \binom{nk-1}{s-1} \left(\frac{b}{z}\right)^{nk}, \quad |z| > b \tag{A6}$$

and

$$W_s = (-1)^s k \sum_{n=0}^{\infty} \binom{nk+s-1}{s-1} \left(\frac{z}{b}\right)^{nk}, \quad |z| < b. \tag{A7}$$

Note that $z = r e^{i\theta}$. Taking the real part of W_s , it follows that

$$U_s = k \sum_{n=1}^{\infty} \binom{nk-1}{s-1} \left(\frac{b}{r}\right)^{nk} \cos nk\theta, \quad r > b \tag{A8}$$

$$U_s = (-1)^s k \sum_{n=0}^{\infty} \binom{nk+s-1}{s-1} \left(\frac{r}{b}\right)^{nk} \cos nk\theta, \quad r < b. \tag{A9}$$

To find the expansion of W_o about $z = b$, we rewrite

$$W_o = -\log(z-b) - \sum_{m=1}^{k-1} \log(z-b e^{2im\pi/k}).$$

Differentiation of W_o s times then gives

$$\frac{d^s W_o}{db^s} = \frac{(s-1)!}{(z-b)^s} + \sum_{m=1}^{k-1} \frac{(s-1)!(e^{2im\pi/k})^s}{(z-b e^{2im\pi/k})^s}.$$

Again,

$$W_s = \frac{b^s}{(s-1)!} \frac{d^s W_o}{db^s} = \frac{b^s}{(z-b)^s} + \sum_{m=1}^{k-1} \frac{(e^{2im\pi/k})^s}{\left(\frac{z}{b} - e^{2im\pi/k}\right)^s}. \tag{A10}$$

Note that $z = b + \zeta$, ζ being a complex variable referred to an origin at $z = b$. It then follows that

$$W_s = \frac{b^s}{\zeta^s} + \sum_{m=1}^{k-1} \frac{(e^{2im\pi/k})^s}{\left(\frac{\zeta}{b} + 1 - e^{2im\pi/k}\right)^s}.$$

Setting $1 - e^{2im\pi/k} = 1/u_m$, we obtain

$$W_s = \frac{b^s}{\zeta^s} + \sum_{n=0}^{\infty} (-1)^n \alpha_s \frac{\zeta^n}{b^n} \tag{A11}$$

where

$$\begin{aligned} \alpha_s &= \binom{n+s-1}{n} \sum_{m=1}^{k-1} (u_m - 1)^s u_m^n \\ &= \binom{n+s-1}{n} \sum_{t=0}^s (-1)^t \binom{s}{t} \sum_{m=1}^{k-1} u_m^{n+s-t} \end{aligned}$$

or

$${}^n\alpha_s = \binom{n+s-1}{n} \sum_{t=0}^s (-1)^t \binom{s}{t} \sigma_{n+s-t} \quad (\text{A12})$$

where

$$\sigma_{n+s-t} = \sum_{m=1}^{k-1} u_m^{n+s-t}. \quad (\text{A13})$$

Setting $\zeta = \rho e^{i\psi}$ in (A11) and taking the real part of W_s , we obtain

$$U_s = \frac{b^s}{\rho^s} \cos s\psi + \sum_{n=0}^{\infty} (-1)^n {}^n\alpha_s \frac{\rho^n}{b^n} \cos n\psi. \quad (\text{A14})$$

Therefore, $\sum_{s=1}^{\infty} C_s U_s$ expressed in terms of (ρ, ψ) coordinates is

$$\sum_{s=1}^{\infty} C_s U_s = \sum_{s=1}^{\infty} {}^o\alpha_s C_s + \sum_{m=1}^{\infty} \left\{ C_m \frac{b^m}{\rho^m} + \left[(-1)^m \sum_{s=1}^{\infty} {}^m\alpha_s C_s \right] \frac{\rho^m}{b^m} \right\} \cos m\psi$$

or

$$\sum_{s=1}^{\infty} C_s U_s = L_o + \sum_{m=1}^{\infty} \left(C_m \frac{b^m}{\rho^m} + L_m \frac{\rho^m}{b^m} \right) \cos m\psi \quad (\text{A15})$$

where

$$L_m = (-1)^m \sum_{s=1}^{\infty} {}^m\alpha_s C_s. \quad (\text{A16})$$

(Received 13 March 1973; revised 7 May 1973)

Абстракт—Даются строгие решения для кручения Сен-Венана круглых труб и сплошных цилиндров, усиленных цилиндрическими включениями из разного материала, одинаково расположенного вокруг концентрического круга. Поставленные проблемы моделируют задачи, которые встречаются в матричных стержнях, усиленных продольными волокнами и, также, в соответствующих задачах железобетона. Получаются формулы для распределений граничных напряжений и жесткостей кручения.

Даются формулы функции напряжений для кручения цилиндров, обладающих многосвязанными, составными сечениями. Применяются две системы полярных координат, используются и периодичность и симметрия. Для подтверждения выводов, вычитываются три вырожденные задачи: соответственное кручение круглой трубы, кольцо круглых стержней и труба с эксцентричными, круглыми отверстиями. Разработано некоторые численные примеры. Даются результаты в виде таблиц и графиков.